Thermal Reactions of $Mo(CO)_6$ on Metal-oxide Surfaces

How-Ghee Ang, Kim-Seng Chan, Gaik-Khuau Chuah, Stephan Jaenicke and Sock-Kim Neo
Department of Chemistry, National University of Singapore, Kent Ridge, Singapore 0511, Republic of Singapore

Temperature-programmed decomposition has been used to determine the energetics of metal–carbonyl bond dissociation in the surface-mediated decarbonylation of $Mo(CO)_6$ adsorbed on alumina, magnesia, silica, titania, zirconia and zinc oxide. To estimate the influence of the surface microstructure, the reaction was studied on a conventional silica gel and on MCM-41, a silica with uniform cylindrical mesopores. Activation energies for successive decarbonylation steps were calculated from the temperature of the desorption maxima using Redhead's equation. The activation energy for the elimination of the first CO from the complex is generally lower than in the gas phase and varies from below 100 kJ mol^{-1} on the basic supports ZnO and MgO, to 126 kJ mol^{-1} on SiO_2. The different microstructure of MCM-41 and a silica with a wide pore-size distribution has no influence on the desorption behaviour. It is proposed that the initial reaction step is the nucleophilic substitution of CO by the free electron pair of a surface O^{2-} or OH group. The electron density at the oxygen is strongly influenced by the adjacent metal cation. An empirical correlation between the activation energy and the field strength at a surface cation site was found to yield a linear relationship. Thus, the decomposition of $Mo(CO)_6$ may be a useful probe for the oxidation state of surface metal ions in simple oxides.

Surface organometallic chemistry[1] is an emerging new field of study. The presence of a surface reduces the dimensionality of a reaction and may open additional reaction channels. In many respects, the surface plays the role of a solvent[2] in stabilizing intermediates and directing the stereochemistry of reactions. In the present study, the interactions of a simple probe molecule, $Mo(CO)_6$, with different oxidic supports have been examined. The influence of the support on the decomposition of metal carbonyls has earlier been observed by the groups of Burwell and Brenner, who studied the thermal reactions of $Mo(CO)_6$ adsorbed on alumina,[3–6] silica[7] and titania.[8] Depending on the support, subcarbonyls, molybdenum metal clusters or low-valent molybdenum species were formed which proved to be active metathesis catalysts.[9] The surface-assisted decomposition of metal carbonyls is also of interest to the semiconductor industry, where refractory metal films are frequently formed by chemical vapour deposition from precursors like $Mo(CO)_6$ and $W(CO)_6$. The laser-induced deposition of molybdenum films from the hexacarbonyl is an autocatalytic process, and the loss of the first CO from the complex seems to be the rate-determining step. The activation energy for the decomposition of $Mo(CO)_6$ was found[10] to be in the order of 80–100 kJ mol^{-1}.

We report here details of the decomposition reactions of $Mo(CO)_6$ on several support materials, namely, γ-Al_2O_3, MgO, TiO_2, ZrO_2, ZnO and two different samples of silica. The silicas studied were a commercial silica gel with a nominal pore diameter of 6 nm and MCM-41, a mesoporous silicate with uniform, non-interconnected cylindrical channels.[11] The material used in this study had pores with a mean diameter of 4.2 nm, with a very narrow distribution. These two different porous silicas were compared with the aim of investigating whether the pore structure affects the reaction path by trapping and retaining the evolved carbon monoxide. This should lead to an observable change in the desorption kinetics if equilibrium reactions between adsorbed subcarbonyl species and CO were involved. Earlier studies of $Mo(CO)_6$ on alumina[6,12] and titania[8] by temperature-programmed decomposition (TPDE) and IR spectroscopy have identified a number of subcarbonyl species as intermediates in the decomposition, and have shown that the degree of surface hydroxylation has considerable influence on the final oxidation state of the molybdenum species. Partially dehydroxylated alumina promotes the formation of molybdena species with the molybdenum in an oxidation state close to 2+, whereas on extensively dehydroxylated surfaces, the decarbonylation leads to metallic molybdenum. Stable subcarbonyls, notably $Mo(CO)_3$, have been observed on alumina at intermediate temperatures, but do not form on silica or titania. In the present study, the energetics of the surface-mediated decomposition reactions have been determined, and an attempt is made to correlate the reaction rates with the surface chemistry of the support.

Temperature programmed decomposition has been developed by Brenner as a tool to study surface reactions of adsorbed carbonyl complexes. This technique is closely related to temperature-programmed desorption (TPD),[13–15] which is widely used to investigate surface properties of heterogeneous catalysts. It is shown that this technique is especially suitable for following the step-wise decomposition of adsorbed molecular entities such as metal carbonyls.

Table 1 Structural properties of the supports used

Support	$S_{BET}/m^2\ g^{-1}$	$V_p/cm^3\ g^{-1}$	d_p (av.)/nm
SiO_2 (MCM-41)	775	0.802	4.2
SiO_2 (Merck)	434	0.834	6.4
TiO_2	31	0.088	12.0
ZrO_2	100	0.167	6.5
γ-Al_2O_3	98	0.247	6.6
MgO	47	0.007	9.5
ZnO	4	—	—

* V_p and d_p are the volume and diameter of the pore respectively.

Experimental

Support materials and their properties are listed in Table 1. γ-Alumina, ZnO, MgO and silica gel (G60, nominal surface area 330 $m^2\ g^{-1}$, average pore size 6 nm) were commercial products (Merck) and used as received. MCM-41 was synthesised

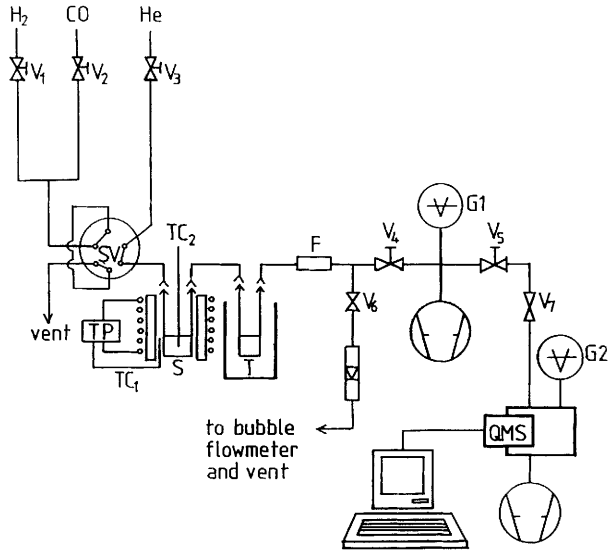

Fig. 1 Schematic diagram of the apparatus used for temperature-programmed decomposition (TPDE); F = 5 μm filter, G_1, G_2 = pressure gauges, QMS = quadrupole mass spectrometer, S = sample, SV = sampling valve, T = trap, TC_1, TC_2 = thermocouples, TP = temperature programmer, V_1–V_6 = fine-metering valves and V_7 = metal-bellow valve (Nupro)

according to the patent disclosure.[16] The synthesis of high surface area ZrO_2 has been described,[17] and TiO_2 was prepared by controlled hydrolysis of $TiCl_4$. Nitrogen adsorption–desorption isotherms were measured with a Micromeritics Flowsorb 2300. The surface areas (S_{BET}) for the various supports were determined according to the Brunauer–Emmett–Teller (BET) theory, and the pore size distributions were calculated from the desorption branch of the isotherms, using the Kelvin equation.[18] All supports were treated for 2 h at 800 K in a flow of high-purity helium immediately before reaction.

The apparatus for the temperature-programmed decomposition (Fig. 1) was modified from a design described earlier.[19] It allows for the continuous monitoring of the evolved carbon monoxide and hydrogen during the preparation of the sample. A stream of helium carrier gas (99.995%, SOXAL) passes over the sample and sweeps the desorbed reaction products through a differentially pumped interface into a quadrupole mass spectrometer (Hiden Analytical, mass range 1–200 au). The reactor, a Pyrex U-tube, can be placed in a cold-bath for the catalyst preparation or in the oven during the decomposition runs. A second U-tube kept at dry-ice temperature was used to trap the solvent and condensable reaction products. For the preparation of the catalysts, $Mo(CO)_6$ (Alpha Chemicals, *ca.* 5 mg) was dissolved in freshly distilled pentane (5 cm^3), then 4 cm^3 of this solution was injected under flowing helium onto the pretreated support (0.25 g for MCM-41, *ca.* 0.50 g for all other supports). The impregnation of the support had to be done directly in the reaction cell, because whereas $Mo(CO)_6$ is air stable, the supported material is easily oxidized by exposure to air. Earlier attempts to prepare a larger batch of the catalyst in a separate vessel and to transfer samples into the reaction cell had therefore failed to give reproducible results. The adsorption reaction was helped by sonicating the slurry for a few minutes; thereafter, the sample was kept at 273 K until all solvent had been removed by trap-to-trap condensation (*ca.* 2–3 h). The mass spectrum of the effluent was continuously monitored during the whole period. Only a small air peak was observed immediately after introduction of the solution. Thus, $Mo(CO)_6$ physisorbs at the preparation temperature as the intact molecule. After all solvent had been removed from the sample, the trap was exchanged for a clean U-tube made from 3 mm internal-diameter tubing. This decreases the dead volume of the system and thereby reduces the broadening of the desorption signals due to back-mixing. The mass spectrometer was then switched to multi-ion detection for mass 2 (H_2) and 28 (CO), and the temperature programme was started. In order to achieve a linear ramp, the oven controller used a thermocouple outside the reactor, while the sample temperature was monitored with a second $\frac{1}{16}$ inch stainless steel sheathed thermocouple. After each run, the amount of gas evolved was calibrated by injections of CO and H_2, using a 6-port valve with a 250 μl sample loop. The pressure gauges G1 and G2 in the differential-pumping stage and in the mass spectrometer chamber, respectively, were essential to establish reproducible conditions for each run. The high background of helium carrier gas (10^{-4} Pa) during the experiments led to an increase in the hydrogen signal in the mass spectrometer. This effect is attributed to stimulated desorption of hydrogen from the metal walls of the vacuum chamber, together with ionization transfer in the ion source. It was therefore not always possible to quantify the hydrogen desorption signal. Activation energies (E_a) were obtained from the temperature at peak maximum, T_p, using the Redhead equation in the form $E_a = RT_p[\ln(\nu T_p/\beta) - 3.46]$, where β is the heating rate in K s^{-1} and ν is the pre-exponential factor (taken as 10^{13} s^{-1}).

Results

The results of the TPDE measurements for the different supports are summarized in Table 2. Brenner and co-workers[5,7] reported earlier that a considerable part of the initially adsorbed hexacarbonyls sublimes from silica and alumina as the intact molecule. This has also been observed for all supports investigated in this study. Molecularly desorbed carbonyl was recovered from the cold trap, and its amount was quantitatively determined by UV spectroscopy. The sublimation losses varied between 15 and 75%, depending on the support and initial loading. Where a comparison is possible, the values reported here for the final loading are in good agreement with Brenner's results except for SiO_2, where we obtained about 10 times higher loadings. This may be related to the narrow pore size of the silica gels used in the present study, compared to the essentially pore-free aerosil or the wide-pore silica gel used in the earlier study. The specific coverage (in molecules per cm^2 surface area) is given in Table 2. It amounts to less than 1% of a monolayer on silica, assuming a monolayer coverage at around 2×10^{14} cm^2, but is considerably higher on TiO_2, MgO and especially on ZnO, where the coverage is close to $\theta = 1$. However, in most cases the coverage is sufficiently low to neglect lateral interactions between adsorbed complexes, and the measurements are interpreted on the basis of a desorption energy which is independent of coverage.

The $Mo(CO)_6$ which remains at the surface undergoes thermal decomposition. Desorption spectra for $Mo(CO)_6$ adsorbed on silica gel, ZrO_2, MgO or γ-alumina are shown in Fig. 2. The spectra can be classified into three different types: on SiO_2 and TiO_2 (not shown), the desorption signal consists of one single narrow peak. On γ-Al_2O_3, ZrO_2 and ZnO, two clearly separated desorption signals are evident. The CO evolution falls to practically zero between the peaks, indicating that a stable subcarbonyl species forms on these surfaces. Finally, on MgO, a well separated peak at lower temperature is followed by a broad signal above 530 K which shows additional structure. Table 2 lists the amount of CO evolved in each peak normalized to the amount of molybdenum. With silica and titania, all six CO are lost almost simultaneously from the complex; the shoulder in the TiO_2 signal indicates a slightly higher activation energy for the loss of the third and subsequent CO than for loss of the first two. For the other supports, an initial loss of three CO leads to a stable surface-bound subcarbonyl $[Mo(CO)_3]_{ads}$, which is presumably stabilized by interaction with O^{2-} or surface OH groups. The remaining three CO are only lost at considerably higher temperature. Hydrogen evolution accomp-

Table 2 TPDE of $Mo(CO)_6$ on different supports

Support	Initial loading (wt%)	Sublimation loss (%)	$Mo(CO)_6$ coverage		T_p/K	CO evolved	CO/Mo	H_2 evolved oxidation state*	
			μmol g^{-1}	10^{-12} molecules cm^{-2}		(μmol g^{-1})		(μmol g^{-1})	
SiO_2 (MCM-41)	2.04	75	19.3	1.45	444.5	114	5.9	1.9	0.2
SiO_2 (Merck)	0.89	64	12.2	1.57	445.5	68.5	5.6	1.4	0.25
TiO_2	1.13	15	36.4	7.0	388	70.5	1.9	Not quantified	
					437.5	142	3.9		
					> 800	12	0.3		
ZrO_2	1.64	14	53.5	32.2	385 (sh)				
					429	161	3.0	—	—
					595.5	161	3.0	41	1.5
γ-A-l_2O_3	1.11	46	22.7	14	387.5	70.8	3.1	—	—
					595.5	65.7	2.9	18.8	1.66
MgO	1.77	39	40.8	52.3	370	127	3.1	Not quantified	
					577	59.8	1.5		
					692.5	60.3	1.5		
ZnO	1.14	65	15.1	228	347	50.1	3.3	Not quantified	
					520	39.9	2.7		

* Final oxidation state of molybdenum at the end of the indicated temperature interval, calculated from evolved hydrogen.

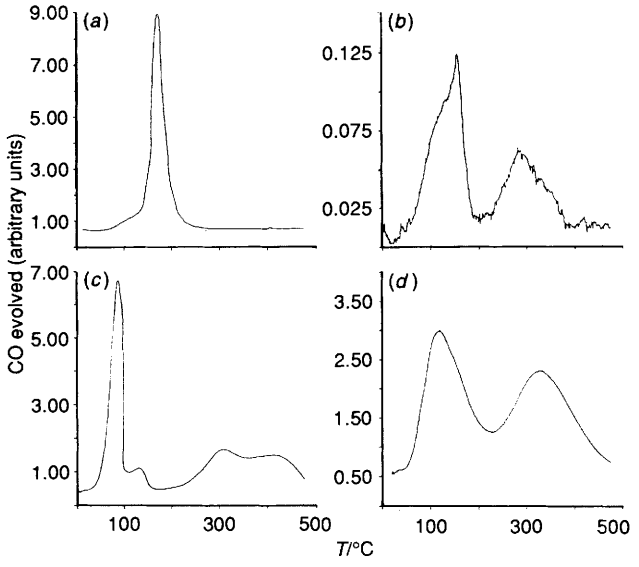

Fig. 2 CO evolution during the TPDE of $Mo(CO)_6$ adsorbed on (*a*) SiO_2 (silica gel), (*b*) ZrO_2, (*c*) MgO or (*d*) γ-Al_2O_3; heating rate = 0.167 K s^{-1} for (*a*)–(*c*), 0.333 K s^{-1} for (*d*)

anies this second CO evolution. This has been observed over partially dehydroxylated supports[8,12] and is consistent with the oxidation of the molybdenum to a final oxidation state around +2. It is not clear whether this indeed indicates the formation of Mo^{2+}, or rather a mixture of Mo^{4+} and metallic molybdenum. Over thoroughly dehydroxylated supports, the thermal decomposition of $Mo(CO)_6$ reportedly leads to metallic molybdenum.[6,8,12] After TPDE, all samples had a dark grey colour, indicative of a highly dispersed metal. However, attempts to determine the metal dispersion by CO chemisorption were inconclusive.

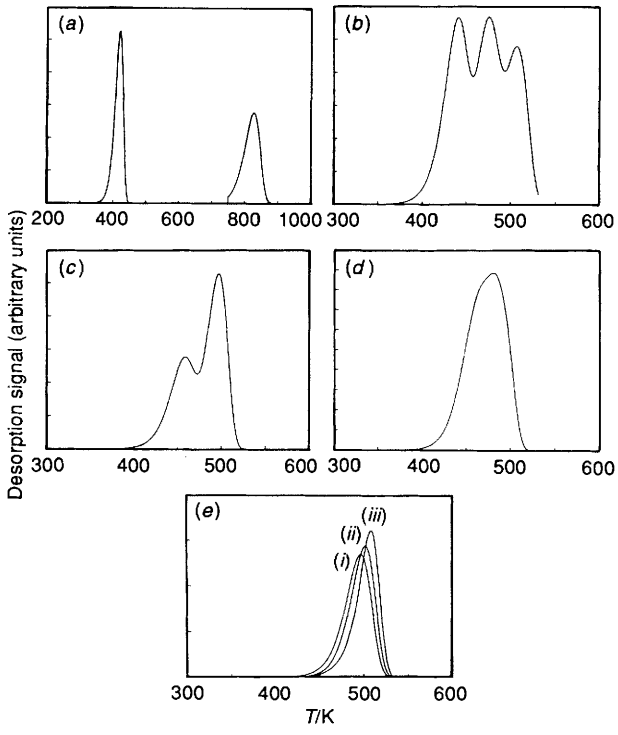

Fig. 3 Simulated temperature-programmed decomposition spectra for CO evolution from an adsorbed metal carbonyl. (*a*) Comparison of the signal for a simple first-order reaction with constant pre-exponential factor and activation energies of 120 (left peak) and 240 kJ mol^{-1} (right peak). (*b*)–(*e*) Spectra for a decomposition reaction with three successive CO-evolution steps; $E_a(1) = 125$, $E_a(2) = 135$ and $E_a(3) = 145$ (*b*); $E_a(1) = 130$ and $E_a(2) = E_a(3) = 140$ (*c*); $E_a(1) = 130$, $E_a(2) = 135$ and $E_a(3) = 140$ (*d*); and (*i*) $E_a(1) = 142$ and $E_a(2) = E_a(3) = 0$, (*ii*) $E_a(1) = E_a(3) = 142$ and $E_a(2) = 130$ and (*iii*) $E_a(1) = E_a(2) = E_a(3) = 142$ kJ mol^{-1} (*e*)

Discussion

The method of temperature-programmed decomposition of surface-adsorbed clusters allows one to determine the stoichiometry of the various surface species present during reactive decarbonylation. In the systems $Mo(CO)_6$–γ-alumina and $Mo(CO)_6$–ZrO_2, a stable subcarbonyl, $[Mo(CO)_3]_{ads}$, is formed. The remaining three CO groups desorb in a second broad peak at around 700 K. On MgO, the reaction leads also initially to the adsorbed tricarbonyl species. Upon further heating, the remaining CO is evolved in at least two peaks. The area of each peak corresponds to a fractional CO/Mo value, indicating that multinuclear subcarbonyl clusters form on this surface. The formation of multinuclear anionic clusters on basic supports like MgO has also been observed by Ugo and co-workers[20] and Gates.[21] On SiO_2, $Mo(CO)_6$ is initially molecularly bound, but decomposes on heating in a single step at *ca.* 444 K. The mesoporous MCM-41 gives very similar results to a conventional silica gel. This indicates that the decomposition mechanism is primarily influenced by the chemical nature of the surface, but not by structural parameters.

A complete analysis of the TPDE spectra yields not only information on the stoichiometry and stability of the surface species, but can be used to gain further insight into the decomposition mechanism of adsorbed metal carbonyls. It had already been recognized by Brenner *et al.*[7] that the TPDE signal of the Group 6 hexacarbonyls from SiO_2 was unexpectedly narrow and indeed in good agreement with the model of a single first-order reaction. It is therefore justified to assume that the much broader signals found on the other supports do not result from surface heterogeneity, but reflect the decomposition kinetics of the adsorbed complex. In order to address the question as to whether TPDE spectra can resolve the different reaction steps, we simulated desorption spectra for a model with successive CO-dissociation steps. A simple Arrhenius behaviour for each desorption step is assumed, $k = \nu \exp(-E_a/kT)$, where ν was taken as 10^{13} s^{-1}. A heating rate of 20 K min^{-1}, similar to that of the experiments, was used for the calculations. Some of the simulated TPDE spectra are reproduced in Fig. 3. The case of a simple first order reaction is shown in Fig. 3(*a*) for two very different activation energies. The desorption signals have the asymmetric shape typical of a first-order reaction. Whereas the signal at higher temperature appears to be broader, it is found that the dimensionless parameter f = (full width at half maximum)/(peak temperature) is almost invariant at 0.067. For the other examples, a model with three consecutive CO losses, simulating the formation of the tricarbonyl species, is considered. If at an activation energy around 120 kJ mol^{-1}, the activation energy for each subsequent step increases by more than 20 kJ mol^{-1} over that of the preceding step, well resolved peaks result. However, if the activation energy for successive steps increases by less than 5 kJ mol^{-1}, individual bands are no longer resolved, but a single broadened desorption signal is obtained. If two successive decomposition reactions with somewhat increasing activation energy are followed by steps with equal or lower activation energy, a shoulder on the low temperature side will result in the desorption spectrum [Fig. 3(*c*)] similar to that observed on ZrO_2 or TiO_2. In Fig. 3(*e*), the three cases are compared: (*i*) the first desorption is rate determining, $E_a(1) \gg E_a(2) = E_a(3)$; (*ii*) the second desorption energy is smaller than the other two, $E_a(1) = E_a(3) > E_a(2)$; and (*iii*) all activation energies are equal, $E_a(1) = E_a(2) = E_a(3)$. Case (*i*) is identical to that of a single first-order reaction. The simulations show that the

Table 3 Activation energies for the CO dissociation $Mo(CO)_n \longrightarrow Mo(CO)_{n-1} + CO$

Support	Rate determining	E_a/kJ mol^{-1}
SiO_2 (MCM-41)	k_1	126.2
SiO_2 (Merck)	k_1	126.5
TiO_2	k_1	109.8
	k_3	124.2
ZrO_2	k_1	110
	k_2	121.7
	k_4	160
γ-Al_2O_3	k_1	108.7
	k_4	170
MgO	k_1	104.5
	k_4	165
	Cluster?	199
ZnO	k_1	97.9
	k_4	148

desorption signal sharpens for (*ii*) and (*iii*). In the case where the three activation energies are equal, the *f* parameter reaches a minimum ($f = 0.055$); it decreases by about 20% compared to the simple first-order reaction. Thus, from a careful line-shape analysis, additional information on the different activation energies may be extracted in the case of sequential reactions.

The experimentally observed signal on silica gel has $f = 0.062$. Thus, it is narrower than predicted for a simple one-step reaction. To appreciate the sharpness of the observed peak, one has to take into account that the experimental signal is somewhat broadened as the result of back-mixing in the dead volume of the reactor and transfer lines. The true linewidth can be obtained by deconvolution with the measured instrument response function. With this correction, the signal will be even sharper than the raw data presented here. Thus, for the decomposition of $Mo(CO)_6$ on silica gel, the situation of case (*iii*) seems to apply, that is, all six bond-breaking steps have a similar activation energy. However, a narrowing of the signal can also be obtained if one assumes a higher frequency factor ν together with a higher activation energy. It can therefore be concluded that on silica, the first CO elimination is the rate-determining step and has the highest activation energy, 126 kJ mol^{-1}, with subsequent CO-elimination reactions having probably only slightly lower activation energies. The activation energies for CO-dissociation from $Mo(CO)_6$ on the different supports are given in Table 3. Where possible, shoulders have been deconvoluted to obtain the activation energies for the different steps. It is estimated that the assumptions on the frequency factor and the influence of overlapping signals introduce an uncertainty of about 10% of the reported values. However, the order of the bond-breaking energies within one system should be reproduced to a much higher accuracy.

Thus, it is found that the presence of the surface has a strong influence on the strength of the Mo–CO bond. Not only is the activation energy for the first CO loss very dependent on the nature of the support, but the support also influences the path of the decomposition reaction. All six carbonyls are lost from $Mo(CO)_6$ in a single step on silica, whereas a multi-step reaction with a number of stable intermediates takes place on MgO. Even in the gas phase, the binding energies of the various CO ligands of a metal carbonyl are not constant. With molybdenum and tungsten hexacarbonyls, the first CO elimination is rate-determining, whereas for chromium hexacarbonyl the intermediate $Cr(CO)_5$ is obtained[22] indicating that the second CO loss is the rate-determining step. Individual bond energies in the gas phase have been determined by ion-cyclotron resonance and kinetic-energy-release distributions.[23] For $Mn(CO)_5$, the first and fourth dissociation energy[24] are around 130 kJ mol^{-1}, while the remaining values are considerably lower, around 80 kJ mol^{-1}. Photo-acoustic calorimetry in solution[25] led to similar results. The gas-phase value[22] of 163 ± 10 kJ mol^{-1} for the rate-determining first CO elimination from $Mo(CO)_6$ or the average value of 150 kJ mol^{-1} calculated from the heat of formation[26] have to be compared to the values found in this study, which vary from 98 to 126 kJ mol^{-1} for the first CO desorption, and reach 200 kJ mol^{-1} for the final CO loss from the carbonyl species adsorbed on MgO. The presence of a solid surface generally reduces the first decomposition energy. It opens new reaction channels and thus can lead to a decrease or increase in the activation energy for subsequent bond dissociations. The chemistry of the surface influences the decomposition mechanism. It had been proposed[12] that the surface-mediated CO elimination from the complex follows a ligand-replacement mechanism, where free electron pairs of oxygen, either from a surface OH group or an O^{2-} ion occupy free co-ordination sites of the metal. The electron density in these oxygen lone pairs will be a function of the 'basicity' of the support, and will be strongly influenced by the field at the neighbouring metal cation. A plot of the activation energy for the first CO loss as a function of the field strength at the surface cations shows indeed a strong correlation (Fig. 4). The cation field strength ('acidity parameter') is expressed as the formal charge (z) divided by the ionic radius of the metal cation (r) in the appropriate co-ordination. While the concept of the field strength of individual ions on a surface is open to criticism,[27] the success of the correlation seems to justify its use in the case of simple metal oxides. Thus, the decomposition reaction of $Mo(CO)_6$ may be a useful probe to estimate the surface charge of metal cations in other supports.

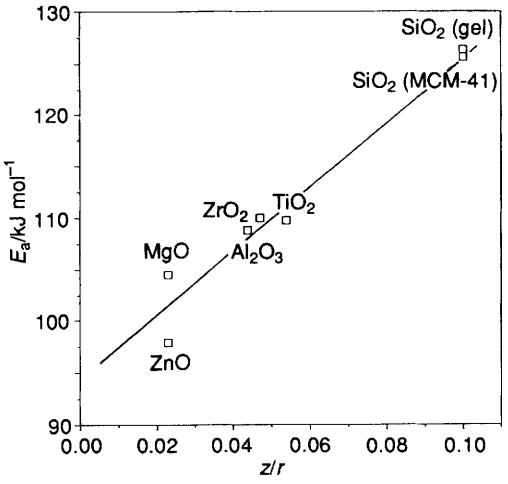

Fig. 4 Correlation between the activation energy E_a for the first CO loss from adsorbed $Mo(CO)_6$ and the field strength at a surface cation site of the support

The results of this investigation show that the surface participates as a 'macroligand' in a reaction with metal organic complexes as proposed by Psaro *et al.*[20] and Gates[21] in their concept of surface organometallic chemistry. 'Acidic' surfaces like SiO_2 and TiO_2 catalyse the decomposition of the carbonyl complex in a single step, leading to highly dispersed metallic molybdenum. More 'nucleophilic' surfaces promote the first CO substitution at a lower temperature than on the acidic surfaces, and stabilize the surface subcarbonyl $[Mo(CO)_3]_{ads}$. The dissociation of the three remaining CO groups takes place only at a much higher temperature, especially for the complexes adsorbed onto MgO. At these high temperatures, the molybdenum is oxidized to an oxidation state close to +2 by reaction with the surface OH groups. A comparison of the two porous silica materials, G60 and MCM-41, reveals that the latter is able to bind more $Mo(CO)_6$. However, if the loading is normalized per unit surface area rather than per unit weight, it is very similar for both types of silica. The desorption signals have an essentially identical shape and the maximum appears at the same temperature. Thus, the surface chemistry on both

types of material is identical. This confirms the observation of Chen *et al.*[28] that MCM-41 has surface properties similar to silica gels, but quite different from those of high-silica zeolites.

Acknowledgements

Support of this research by the National University of Singapore (RP940602) is gratefully acknowledged. We thank Dr. Ch. Zybill (National University of Singapore) and Dr. Yu. Suchorski (Fritz–Haber–Institute, Berlin) for helpful discussions.

References

1 *J. Mol. Catal.*, 1994, **86**.
2 H. H. Lamb, B. C. Gates and H. Knözinger, *Angew. Chem., Int. Ed. Engl.*, 1988, **27**, 1127.
3 A. Brenner and R. L. Burwell, jun., *J. Am. Chem. Soc.*, 1975, **97**, 2565.
4 R. L. Burwell, jun., and A. Brenner, *J. Mol. Catal.*, 1976, **1**, 77.
5 A. Brenner and R. L. Burwell, jun., *J. Catal.*, 1978, **52**, 353.
6 R. Nakamura, D. Pioch, R. G. Bowman and R. L. Burwell, jun., *J. Catal.*, 1985, **93**, 388, 399.
7 A. Brenner, D. A. Hucul and S. J. Hardwick, *Inorg. Chem.*, 1979, **18**, 1487.
8 P. N. Gonzales, M. A. Villa Garcia and A. Brenner, *J. Catal.*, 1989, **118**, 360.
9 R. L. Banks and G. C. Bailey, *Ind. Eng. Chem. Prod. Res. Dev.*, 1964, **3**, 170.
10 F. A. Houle and L. I. Yeh, *J. Phys. Chem.*, 1992, **96**, 2691.
11 C. T. Kresge, M. E. Leonowicz, W. J. Roth, J. C. Vartuli and J. S. Beck, *Nature*, 1992, **359**, 710.
12 J. Goldwasser, S. M. Fang, M. Houalla and W. K. Hall, *J. Catal.*, 1989, **115**, 34.
13 R. J. Cvetanovic and Y. Amenomiya, *Adv. Catal.*, 1967, **17**, 103.
14 R. J. Cvetanovic and Y. Amenomiya, *Catal. Rev.*, 1972, **6**, 21.
15 J. L. Falconer and J. A. Schwarz, *Catal. Rev. Sci. Eng.*, 1983, **25**, 141.
16 Mobil Corporation, *US Pat.*, 5 098 684, 1992; 5 108 725, 1992.
17 K. S. Chan, G. K. Chuah and S. Jaenicke, *J. Mater. Sci. Lett.*, 1994, **13**, 1579.
18 S. J. Gregg and K. S. W. Sing, *Adsorption, Surface Area and Porosity*, Academic Press, London, 1982.
19 H. G. Ang, G. K. Chuah and S. Jaenicke, in *Recent Advances in Inorganic and Organometallic Chemistry*, Proceedings of the JSPS–NUS Joint Seminar on Inorganic and Organometallic Chemistry, eds. R. Okazaki and H. G. Ang, Tokyo University Press, 1994, p. 149.
20 R. Psaro, D. Roberto, R. Ugo, C. Dossi and A. Fusi, *J. Mol. Catal.*, 1992, **74**, 391.
21 B. C. Gates, *J. Mol. Catal.*, 1994, **86**, 95.
22 K. E. Lewis, D. M. Golden and G. P. Smith, *J. Am. Chem. Soc.*, 1984, **106**, 3905.
23 *ACS Symp. Ser.*, 1990, **428** and refs. therein.
24 P. A. M. van Koppen, M. T. Bowers, J. L. Beauchamp and D. D. Dearden, *ACS Symp. Ser.*, 1990, **428**, 3.
25 J. K. Klassen, M. Selke, A. A. Sorensen and G. K. Yang, *ACS Symp. Ser.*, 1990, **428**, 195.
26 J. A. Connor, *Top. Curr. Chem.*, 1977, **71**, 71.
27 Yu. Suchorski, W. A. Schmidt, N. Ernst, J. H. Block and H. J. Kreuzer, *Prog. Surf. Sci.*, 1995, **48**, 121.
28 C.-Y. Chen, H.-X. Li and M. E. Davis, *Microporous Mater.*, 1993, **2**, 17; 27.

Received 23*rd March* 1995; *Paper* 5/01881A